

Usefulness of the Burnett Description of Strong Shock Waves

E. Salomons and M. Mareschal

Centre Européen de Calcul Atomique et Moléculaire, Université Paris-Sud, Bâtiment 506, 91405 Orsay CEDEX, France
(Received 24 February 1992)

Atomistic simulations of a strong shock wave in a hard-sphere gas are analyzed in terms of thermodynamic forces and fluxes. Evidence is provided that the Burnett corrections to the heat flux significantly improve the agreement with the computed values over the Navier-Stokes predictions in the shock-front region.

PACS numbers: 47.40.Nm, 47.45.-n, 51.10.+y

A plane shock wave in a fluid [1-3] is known to be inaccurately described by the Navier-Stokes equations of fluid dynamics; in the case of a gas, deviations occur already for Mach numbers $M \geq 2$ (see, e.g., [4]). The Navier-Stokes equations represent a continuum theory based on linear relations between thermodynamic forces and fluxes. These relations are known as the linear laws: Newton's law of friction and Fourier's law of heat conduction. In a strong shock wave, the forces, i.e., gradients in hydrodynamic densities, are large, and the failure of the Navier-Stokes equations can be attributed to deviations from the linear laws.

For the case of a dilute gas, more general relations between thermodynamic forces and fluxes have been derived from perturbation expansions of the solution of Boltzmann's equation [5]. A well-known expansion is the Chapman-Enskog expansion [6], which yields the so-called Burnett equations when second-order terms (both products of gradients and second-order derivatives) are retained. Although doubts have been raised concerning the mathematical validity of the Burnett equations [7-9], an important question is whether they give a better description of fluid flow with large gradients, such as a shock wave.

In this Letter we present atomistic-simulation results for the local fluxes and forces in strong shock waves in a hard-sphere gas. For Mach numbers between $M=4$ and $M=134$, we find that, in the region of the shock front, the viscous parts of the longitudinal and transverse momentum fluxes (i.e., components of the pressure tensor) are about 30% larger than expected from Newton's law of friction, and that the heat flux is about 70% larger than expected from Fourier's law of heat conduction. We demonstrate that the comparison is considerably improved by adding the Burnett corrections to the linear laws.

For the simulation of a hard-sphere gas we use two techniques. First, we use the molecular-dynamics (MD) method, i.e., direct integration of the equations of motion of the atoms [10]. Second, we use the direct simulation Monte Carlo (DSMC) method [11-13], a powerful technique which is widely used in rarefied gas dynamics (see, e.g., [14]). The DSMC method gives a stochastic solution of Boltzmann's equation, in the sense that it uses the same assumptions that are implicit in Boltzmann's equation

(in particular, the *stosszahlansatz*) [15]. We find that MD and DSMC results are in good agreement with each other, even for a shock wave with Mach number $M=134$.

As far as we know, MD simulations of shock waves in a gas have not been reported before in the literature. MD simulations of shock waves in a liquid have been reported, showing density profiles with small but significant deviations from Navier-Stokes profiles [16-18]. While our work was inspired by this work on liquids, a major reason for studying a dilute gas was to investigate the accuracy of the Burnett equations.

For the description of a plane shock wave one can use a fixed laboratory frame, in which the shock front moves into a gas at rest. It is, however, more convenient to use a moving frame, in which the shock front is fixed. In this frame the shock wave has a steady profile, so that the hydrodynamic fluxes

$$\rho u \quad (\text{mass flux}), \quad (1a)$$

$$P_{xx} + \rho u^2 \quad (\text{momentum flux}), \quad (1b)$$

$$(e + \frac{1}{2} u^2) \rho u + P_{xx} u + J_{Q,x} \quad (\text{energy flux}) \quad (1c)$$

are constant, i.e., independent of position and time. Here ρ is the mass density, u is the x component of the stream velocity (i.e., the component in the direction of the shock wave), P_{xx} is the longitudinal component of the pressure tensor, e is the internal energy per mass unit (excluding kinetic energy relative to the fluid stream), and $J_{Q,x}$ is the x component of the heat flux.

Far from the shock front the heat flux $J_{Q,x}$ vanishes, and P_{xx} is equal to the hydrostatic pressure p . This leads to the Hugoniot relations between the gas properties in the unshocked (indicated by index 0) and shocked (index 1) regions:

$$\rho_0 u_0 = \rho_1 u_1, \quad (2a)$$

$$\rho_0 + \rho_0 u_0^2 = \rho_1 + \rho_1 u_1^2, \quad (2b)$$

$$e_0 + \frac{1}{2} u_0^2 + p_0/\rho_0 = e_1 + \frac{1}{2} u_1^2 + p_1/\rho_1. \quad (2c)$$

In addition, the equation of state and the energy function are known. Here we consider a monatomic hard-sphere gas, with density small enough for use of the ideal-gas law, so that $p = nk_B T$ ($n \equiv \rho/m$, m is the mass of a mole-

cule) and $e = \frac{3}{2} k_B T/m$. The Mach number is defined as $M = u_0/a_0$, where a denotes the speed of sound.

To compute the full profiles $\rho(x)$, $u(x)$, and $T(x)$ from conservation of hydrodynamic fluxes (1), one introduces the linear laws. Newton's law of friction gives for the longitudinal and transverse components of the pressure tensor

$$P_{xx}(x) = p(x) - \left[\frac{4}{3} \eta(x) + \zeta(x) \right] \frac{du(x)}{dx}, \quad (3a)$$

$$P_{yy}(x) = p(x) + \left[\frac{2}{3} \eta(x) - \zeta(x) \right] \frac{du(x)}{dx}, \quad (3b)$$

where $\eta = (5/16\sigma^2)(mk_B T/\pi)^{1/2}$ is the shear viscosity of a gas of hard spheres with diameter σ , and the bulk viscosity ζ is zero for an ideal gas [6]. Fourier's law of heat conduction is

$$J_{Q,x} = -\kappa \frac{dT(x)}{dx}, \quad (4)$$

where $\kappa = (25c_V/32\sigma^2)(mk_B T/\pi)^{1/2}$ is the thermal conductivity [6]. The profiles are now easily obtained by integration starting from the high-density side of the shock wave [17,19].

In our simulations, we use number densities in the region from 3×10^{25} to $1.2 \times 10^{26} \text{ m}^{-3}$. These densities lie in the narrow region where the MD method and the DSMC method can be compared and still be used at a reasonable cost.

Before the results are presented, some details of the simulations are given. The presentation is restricted to a shock wave with Mach number $M = 134$, but it should be noted that we also performed simulations for $M = 10.8$ and $M = 4.6$, which gave qualitatively similar results as for $M = 134$.

For the MD simulations the equations of motion of the molecules are integrated by the method described in Ref. [10]. Since we are dealing with hard spheres, the dynamics consists of a succession of elastic collisions. A rectangular simulation box is used, with dimensions along the x , y , and z axes of $70 \times 10^{-8} \text{ m}$, 0.57×10^{-8} , and 0.57×10^{-8} , respectively. For efficient computation of collision times, the system is divided into 500 cells along the x axis. Collisions with image particles are restricted to nearest image cells by treating cell boundaries as virtual collision partners. Since we want to simulate a steady flow, particles are injected and removed at the two system boundaries normal to the x axis. Time intervals between successive injections are computed from the following expression for the inward flux J_i in the direction of the stream velocity u in an equilibrium gas [11]:

$$J_i = n(k_B T/2\pi m)^{1/2} [\exp(-s^2) + s\sqrt{\pi}\{1 + \text{erf}(s)\}], \quad (5)$$

with $s = u/(2k_B T/m)^{1/2}$. Values of n , u , and T at the two boundaries should be selected in accordance with the Hugoniot relations (2). For the simulation with Mach number $M = 134$, the number of particles was around

$N = 2000$, and the simulation time was $0.6 \times 10^{-9} \text{ s}$, including $0.2 \times 10^{-9} \text{ s}$ for reaching the steady state (step functions were used as initial profiles).

The DSMC method is an approximate, but computationally fast, method of calculating the dynamics of a molecular system. The basic approximation is the uncoupling, over a small time step (small compared with the mean collision time of the molecules), of the motion and the collisions of the molecules. The system is again divided into cells, with linear dimensions small compared with the mean free path of the molecules. A Monte Carlo (i.e., random) procedure is employed to select, for each cell, a representative set of collisions appropriate to the time interval (for more details, see Refs. [12,13]). For the simulation with Mach number $M = 134$, the number of hard-sphere molecules was around $N = 20000$, a simu-

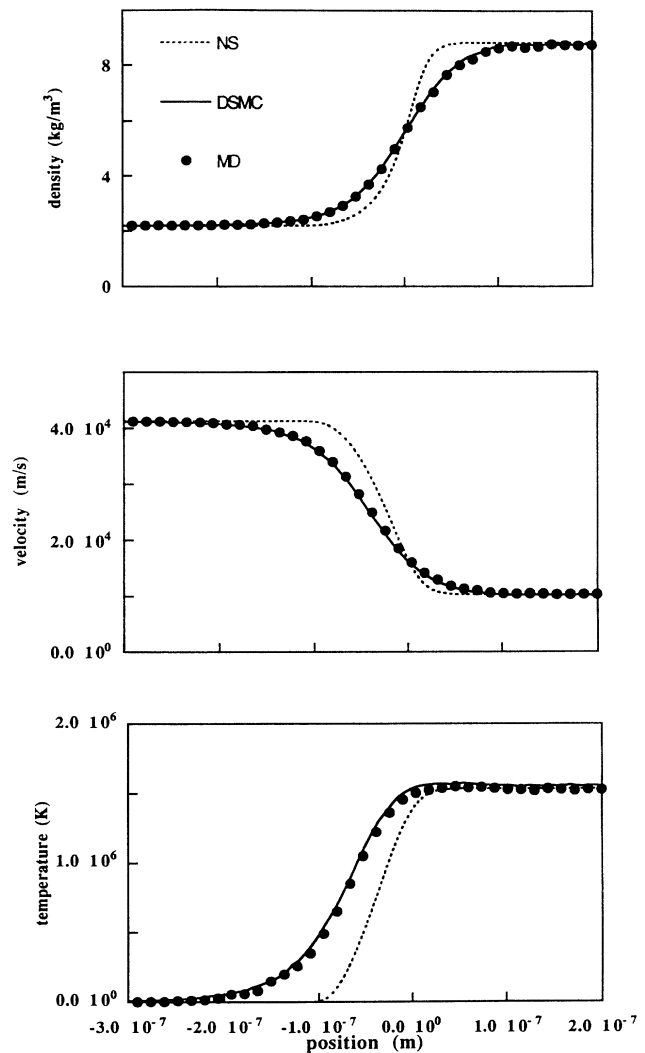


FIG. 1. Profiles $\rho(x)$, $u(x)$, and $T(x)$ for a shock wave with Mach number $M = 134$, obtained by MD (solid circles), DSMC (solid lines), and Navier-Stokes equations (dotted lines).

lution box of length 70×10^{-8} m was used (the y and z directions are irrelevant for the DSMC method in a one-dimensional problem), the number of cells was 500, the time step was 10^{-14} s, and the total simulation time was the same as for the MD simulation. Flux conditions at the boundaries were obtained by replacing, after each time step, all molecules in the first and the last cell by new molecules with velocities selected from the appropriate Maxwellians.

In Fig. 1 simulation results are presented for the density, velocity, and temperature profiles of a shock wave with Mach number $M=134$. MD and DSMC profiles are in good mutual agreement. For comparison, Navier-Stokes profiles are also included in Fig. 1. Both the MD and DSMC temperature profiles are nonmonotonic, with a maximum near position $x=0$. This is not an artifact of the simulations, but has been observed also in accurate numerical solutions of the Boltzmann equation [20]. It is concluded that our simulation results are accurate, and also that the DSMC method provides a good approximation for a strong shock wave at the densities we have used.

Figure 1 clearly demonstrates the well-known fact that the Navier-Stokes equations fail for a shock wave with Mach number $M \geq 2$. We will now demonstrate quantitatively how this failure corresponds to local deviations from the linear laws, which form the basis of the Navier-Stokes equations. In Fig. 2, MD and DSMC profiles of hydrodynamic fluxes are presented: the viscous parts (i.e., excluding the hydrostatic pressure) of the longitudinal and transverse momentum flux, and the heat flux. Also included in Fig. 2 are the profiles predicted by the linear laws (3) and (4), with hydrodynamic forces obtained by numerical differentiation of the MD and DSMC velocity and temperature profiles. The extrema in the momentum-flux profiles are about 30% larger than expected from Newton's law of friction. The minimum in the heat-flux profile is about 70% larger than expected from Fourier's law. In addition, the flux profiles are slightly shifted with respect to the profiles predicted from the forces. It should be noted that deviations from the

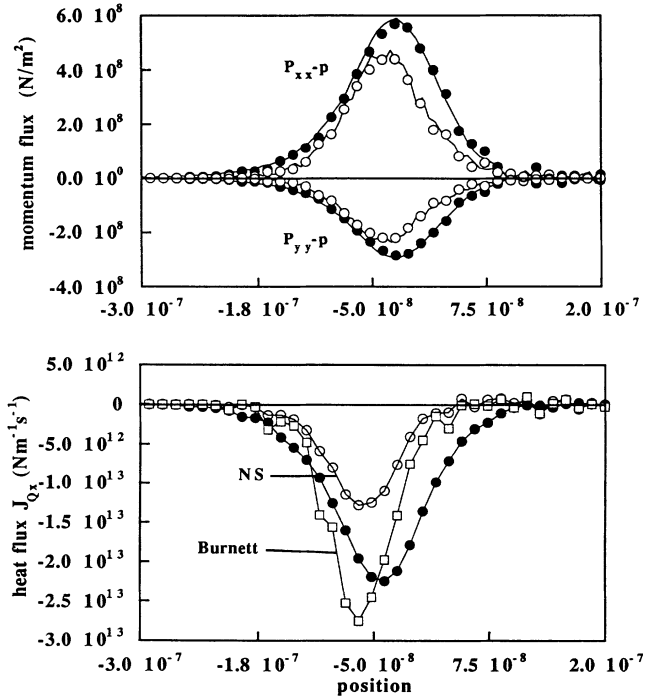


FIG. 2. Profiles $P_{xx}(x)-p(x)$, $P_{yy}(x)-p(x)$, and $J_{Q,x}(x)$ for a shock wave with Mach number $M=134$ (the position scale is the same as in Fig. 1), obtained by MD (symbols) and DSMC (lines). Solid circles represent directly computed fluxes, open circles represent values predicted by the linear laws (3) and (4), and squares represent values including the Burnett correction (6).

ideal-gas values of the transport coefficients η , ζ , and κ are easily verified to be negligible for the density range used here [7]. We believe that we have performed an accurate determination of the deviations from the linear laws for a shock wave. The accuracy is confirmed by the agreement of MD and DSMC values in Fig. 2.

Now, we look at the adequacy of the Burnett equations to account for the deviations from the linear laws. The Burnett correction to the heat flux is [21], for the present geometry,

$$J_{Q,x}^{(2)} = \frac{\eta^2}{\rho} \left[\frac{12.89}{T} \left(\frac{du}{dx} \right) \left(\frac{dT}{dx} \right) - 2.27 \left(\frac{d^2u}{dx^2} \right) - \frac{2.06}{p} \left(\frac{dp}{dx} \right) \left(\frac{du}{dx} \right) \right]. \quad (6)$$

Adding this correction to the values predicted by Fourier's law substantially improves the comparison with the directly computed heat flux (see Fig. 2). We tried to compute also the Burnett correction for the momentum flux [6,21], but unfortunately the statistical scatter in the simulation values is not small enough to allow an accurate determination of second-order derivatives [the momentum-flux correction contains important contributions from second-order derivatives, whereas the second-order derivative in the heat-flux correction (6) is small compared with the other two terms]. If a full hydro-

dynamic calculation including the Burnett terms would be possible, the enhanced hydrodynamic fluxes might give a larger shock-wave thickness, in better agreement with the simulations (see Fig. 1).

It should be noted that the improvement obtained by the Burnett correction to Fourier's law does not imply anything concerning the mathematical validity of the Burnett equations. However, the improvement does imply that the corresponding approximation of the distribution function gives a reasonable description of a fluid sub-

ject to large gradients.

We are grateful to Professor G. Ciccotti and Dr. S. Succi for valuable discussions. The "Fonds National de la Recherche Scientifique" (Belgium) is acknowledged for financial support for one of us (M.M.).

-
- [1] J. O. Hirschfelder, C. F. Curtis, and R. B. Bird, *Molecular Theory of Gases and Liquids* (Wiley, New York, 1954), pp. 783–792.
- [2] Ya. B. Zel'dovich and Yu. P. Raizer, *Physics of Shock Waves and High-Temperature Hydrodynamic Phenomena* (Academic, New York, 1966), Vol. 1, pp. 45–69.
- [3] L. D. Landau and E. M. Lifshitz, *Fluid Mechanics*, Course of Theoretical Physics Vol. 6 (Pergamon, Oxford, 1959), pp. 310–346.
- [4] H. W. Liepmann, R. Narasimha, and M. T. Chahine, *Phys. Fluids* **5**, 1313 (1962).
- [5] H. Grad, in *Handbuch der Physik*, edited by S. Flügge (Springer, Berlin, 1958), Vol. 12, pp. 205–302.
- [6] S. Chapman and T. G. Cowling, *The Mathematical Theory of Non-Uniform Gases* (Cambridge Univ. Press, Cambridge, 1960), pp. 259–272.
- [7] P. Résibois and M. de Leener, *Classical Kinetic Theory of Fluids* (Wiley, New York, 1977), pp. 98–105 and 360–364.
- [8] I. Prigogine, *Physica (Utrecht)* **15**, 271 (1949).
- [9] J. Ford and G. W. Foch, in *Studies in Statistical Mechanics*, edited by J. de Boer and G. E. Uhlenbeck (North-Holland, Amsterdam, 1970), Vol. 5, pp. 103–191.
- [10] M. P. Allen and D. J. Tildesley, *Computer Simulation of Liquids* (Clarendon, Oxford, 1987), pp. 101–109.
- [11] G. A. Bird, *Molecular Gas Dynamics* (Clarendon, Oxford, 1976), pp. 118–142.
- [12] G. A. Bird, in "Microscopic Simulations of Complex Hydrodynamic Phenomena," Proceedings of the NATO ASI Summer School, Alghero, Sardinia, July 1991 (to be published).
- [13] G. A. Bird, *Prog. Astronaut. Aeronaut.* **118**, 211 (1989).
- [14] J. N. Moss, in *Proceedings of the Fifteenth International Symposium on Rarefied Gas Dynamics, 16–20 June 1986, Grado, Italy*, edited by V. Boffi and C. Cergignani (Teubner, Stuttgart, 1986), p. 384.
- [15] S. Harris, *An Introduction to the Theory of the Boltzmann Equation* (Holt, Rinehart and Winston, New York, 1971), pp. 203–205.
- [16] W. G. Hoover, *Phys. Rev. Lett.* **42**, 1531 (1979).
- [17] B. L. Holian, W. G. Hoover, B. Moran, and G. K. Straub, *Phys. Rev. A* **22**, 2798 (1980).
- [18] B. L. Holian, in "Microscopic Simulations of Complex Hydrodynamic Phenomena" (Ref. [12]).
- [19] D. Gilbarg and D. Paolucci, *J. Rat. Mech. Anal.* **2**, 617 (1953).
- [20] S. M. Yen, *Annu. Rev. Fluid Mech.* **16**, 67 (1984).
- [21] C. S. Wang Chang and G. E. Uhlenbeck, in *Studies in Statistical Mechanics* (Ref. [9]), Vol. 5, pp. 8–10.